Available online at www.sciencedirect.com
ScienceDirect
Cement and Concrete Research 36 (2006) 1744–1751
Cement and Concrete Research

Influence of polymer on cement hydration in SBR-modified cement pastes

Ru Wang *, Xin-Gui Li, Pei-Ming Wang

Key Laboratory of Advanced Civil Engineering Materials, Ministry of Education, School of Materials Science and Engineering, Tongji University, 1239 Siping Road, Shanghai 200092, China
Institute of Cement-Based Materials, School of Materials Science and Engineering, Tongji University, 1239 Siping Road, Shanghai 200092, China

Received 21 January 2005; accepted 29 May 2006

Abstract

The influence of styrene–butadiene rubber (SBR) latex on cement hydrates $Ca(OH)_2$, ettringite, C_4AH_{13} and C–S–H gel and the degree of cement hydration is studied by means of several measure methods. The results of DSC and XRD show that the $Ca(OH)_2$ content in wet-cured SBR-modified cement pastes increases with polymer–cement ratio (*P*/*C*) and reaches a maximum when *P*/*C* is 5%, 10% and 10% for the pastes hydrated for 3 d, 7 d and 28 d, respectively. With wet cure, appropriate addition of SBR promotes the hydration of cement, while the effect of SBR on the content of $Ca(OH)_2$ and the degree of cement hydration is not remarkable in mixed-cured SBR-modified cement pastes. XRD results illustrate that SBR accelerates the reaction of calcium aluminate with gypsum, and thus enhances the formation and stability of the ettringite and inhibits the formation of C_4AH_{13}. The structure of aluminum-oxide and silicon-oxide polyhedron is characterized by ^{27}Al and ^{29}Si solid state NMR spectrum method, which shows that tetrahedron and octahedron are the main forms of aluminum-oxide polyhedrons in SBR-modified cement pastes. There are only $[SiO_4]^{4-}$ tetrahedron monomer and dimer in the modified pastes hydrated for 3 d, but there appears three-tetrahedron polymer in the modified pastes hydrated for 28 d. The effect of low SBR dosage on the structure of aluminum-oxide and silicon-oxide polyhedron is slight. However, the combination of Al^{3+} with $[SiO_4]^{4-}$ is restrained when *P*/*C* is above 15%, and the structure of Al^{3+} is changed obviously. Meantime, the polymerization of the $[SiO_4]^{4-}$ tetrahedron in C–S–H gel is controlled.

Keywords: SBR-modified cement paste; Hydrate; DSC; XRD; NMR

1. Introduction

Polymer-modified mortar and concrete are good repair materials for construction in most conditions for their excellent physical and mechanical properties and durability [1–3]. It was reported that the property improvement of mortar and concrete by polymer modification was related to the influence of polymer on the material structures, cement hydration, porosity and unit water content, and also to the chemical and physical interactions between the polymers and cement hydrates [4–10]. However, the polymer modification mechanism is unclear, which confines further development of polymer modified cementitious materials.

Styrene–butadiene rubber (SBR) latex has been widely used to significantly modify mortar. Previous results showed that SBR-modified mortar had good mechanical properties [11,12], anti-penetrability [13,14] and frost resistance [15]. A late report exhibited that SBR could be used to make self-leveling materials [16]. Our earlier work indicated that SBR could reduce water requirement, effectively enhance both flexural strength and tensile bond strength, substantially decrease the ratio of compressive strength to flexural strength, and improve the ratio of flexural strength to elastic modulus. The prepared SBR-modified mortar is suitable for bridge repair [17,18]. With same water–cement ratio (*W*/*C*), the compressive and flexural strengths of SBR-modified mortars are directly proportional to its apparent bulk density at polymer–cement ratio (*P*/*C*) below 10% [19]. Inter-penetrating structures of polymer and cement hydrates formed in SBR-modified mortars, and the interface structures and anti-cracking property of the cement mortar are improved by SBR modification [20].

It was reported that SBR retarded the early hydration reaction of cement in SBR-modified cement pastes but had no effect on the degree of cement hydration at long curing age by hydration heat, chemical combined water content and

* Corresponding author. Tel.: +86 21 6598 0526; fax: +86 21 6598 5385.
E-mail addresses: wr_irene@163.com, ruwang@mail.tongji.edu.cn (R. Wang).

0008-8846/$ - see front matter © 2006 Elsevier Ltd. All rights reserved.
doi:10.1016/j.cemconres.2006.05.020

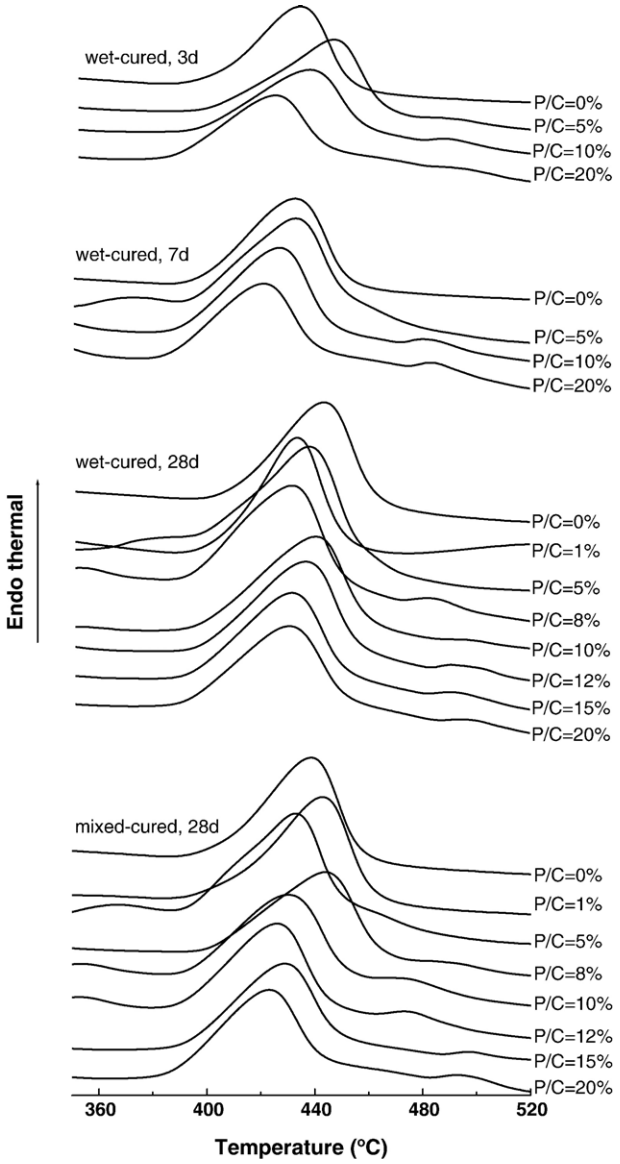

Fig. 1. DSC curves of SBR-modified cement pastes.

differential scanning calorimetry (DSC) analysis [8]. In this paper, several important techniques including DSC, X-ray diffraction (XRD), ^{27}Al and ^{29}Si solid state nuclear magnetic resonance (NMR) were used to research the effect of SBR on cement hydrates $Ca(OH)_2$, ettringite, C_4AH_{13}, C–S–H gel and the degree of cement hydration to provide a basis for polymer modification mechanism.

2. Experimental

2.1. Materials

Portland cement type P II 52.5R, according to Chinese Standard GB 175, was used for preparing the specimens. The chemical compositions and physical properties of the cement are the same with those used in previous paper [19]. The Styrofan SD622S SBR latex (viscosity: 30 mPa·s (20 °C); Tg: 11 °C; pH: 9.5 (20 °C); solid content: 47%) and deionized water were used in the experiment.

2.2. Specimen preparation

The paste specimens were prepared with *P*/*C* of 0–20%, *W*/*C* of 0.40. The polymer latex was added to water firstly, and then specimens 20 × 20 × 20 mm were prepared after the fresh paste was mixed round according to Chinese Standard GB/T 1346-2001. The specimens were demolded after being cured at 20 °C/90 ± 5% R.H. for 24 h, and subsequently were cured for 2 d, 6 d or 27 d immersed in 20 °C water (wet cure) or 6d immersed in 20 °C water followed by 21d at 20 °C and 70 ± 5% R.H. (mixed cure). The samples, taken at a depth of > 1 mm from the surfaces of the cured specimens, were broken into pieces and cleaned with pure alcohol, and then stored in alcohol for at least 6 d for hydration interruption. Before tested, the pieces were removed from the alcohol and vacuum-oven-dried until the mass becomes constant. The powder for DSC, XRD, ^{27}Al NMR and ^{29}Si NMR measurement was obtained by grinding of the dried pieces with FRISCH Puluerisette 7 Planetary Micro Mill.

2.3. Measure technologies

2.3.1. DSC analysis

DSC measurements of the samples were performed by heating from 30 °C to 700 °C at an increasing temperature rate of 20 °C·min^{-1} under a nitrogen atmosphere, by using a NETZSCH STA 449C differential scanning calorimeter.

2.3.2. XRD analysis

The XRD curves were measured with a graphite-monochromatized CuKα radiation generated at 40 kV and 200 mA in a Rigaku D/max 2550 X-ray diffractometer. FT scanning was carried out at 2θ range of 8–13° and 17–19°, respectively. The step length is 0.02°, and the settle time of every step is 6 s at 8–13° and 3 s at 17–19°.

2.3.3. ^{27}Al and ^{29}Si NMR analysis

^{27}Al and ^{29}Si NMR spectra were obtained with a Bruker AVANCE 400 (SB) nuclear magnetic resonance spectrometer with a 4 mm/15 kHz solid CP/MAS explorer. The center

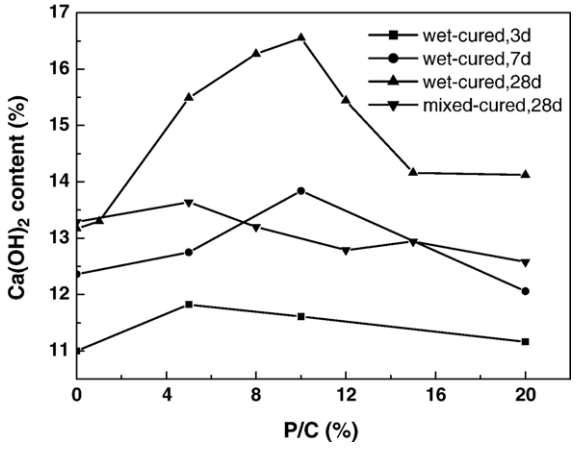

Fig. 2. Relationship between the $Ca(OH)_2$ content and *P*/*C* in SBR-modified cement pastes.

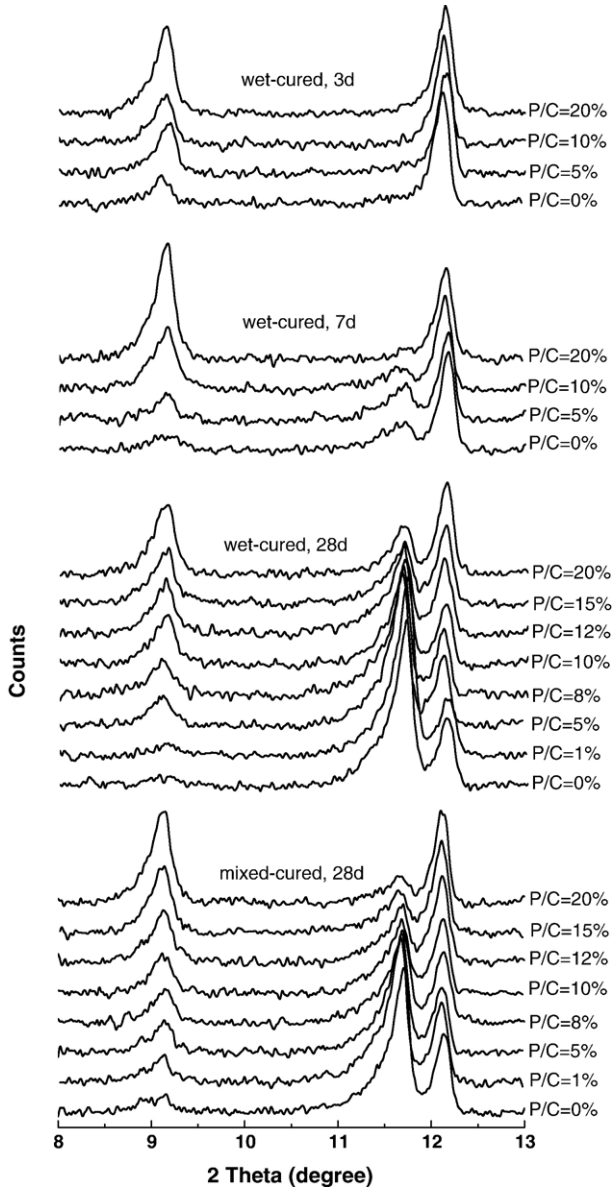

Fig. 3. XRD curves of SBR-modified cement pastes at 2θ range of 8–13°.

frequency of ^{27}Al and ^{29}Si is 104.26 and 79.49 MHz, rotation speed of the sample is 9 and 5 kHz, pulse time is 0.75 and 4.5 μs, retard time is 0.5 and 1.5 s for ^{27}Al and ^{29}Si, respectively, and the pulse energy is 2 dB.

3. Results and discussion

3.1. DSC analysis

$Ca(OH)_2$ is one of the important cement hydrates. Its content differs and can be up to 25% according to chemical compositions of the cement, hydration time and condition. Previous researches proved that the degree of cement hydration calculated based on the content of $Ca(OH)_2$ measured with DSC is credible [21,22]. Fig. 1 shows the DSC curves of SBR-modified cement pastes hydrated for different ages at different conditions. The content of the $Ca(OH)_2$ in the modified pastes is calculated according to Eq. (1) based on the enthalpy of decomposition reaction of analytical pure Ca $(OH)_2$ and that of $Ca(OH)_2$ in the modified pastes. The results are shown in Fig. 2. The $Ca(OH)_2$ content in wet-cured modified pastes with different ages augments with P/C, and then reduces after reaching a maximum. The longer the curing age, the more obvious the variation. It indicates that the degree of cement hydration in wet-cured SBR-modified cement pastes increases with P/C firstly and then declines. The degree of cement hydration reaches a maximum when P/C is 5% for the modified pastes hydrated for 3 d, 10% for the pastes hydrated for 7 d and 28 d. The change of the degree of cement hydration with P/C is due to the formation of polymer film in the pastes. When P/C is below 10%, the latex and cement mix perfectly and there is no much polymer accumulation [20], which allows free transfer of ions in the system. Meantime, polymer phase keeps some water in itself and provides water for cement hydration successively, which results in the maximum of the degree of cement hydration change to higher P/C with curing time. However, when P/C is higher, the formed polymer film in the paste becomes thicker, which limits the transfer of ions, and thus prevents further cement hydration. The content of Ca $(OH)_2$ decreases slightly with P/C in mixed-cured SBR-modified cement pastes, which suggests that the effect of SBR on the degree of cement hydration is not obvious at mixed-curing condition. The difference in the degree of cement hydration between the two curing methods is due to that wet cure can keep water in the cement pastes, which is helpful for cement hydration; while under mixed cure, the water in the

Table 1
The integrated results of XRD diffraction peak of (100) crystal plane of ettringite

	P/C	d-value (Å)	FWHM (°)	Max. int.	Integ. int.	$\frac{\text{Integ.int.}(1+P/C)}{\text{Integ.int}_{P/C=0}}$
Wet-cured, 3 d	0	9.719	0.223	96	32.09	1.00
	0.05	9.611	0.273	162	50.96	1.67
	0.10	9.670	0.239	156	49.65	1.70
	0.20	9.659	0.235	285	86.60	3.24
Wet-cured, 7 d	0	9.583	0.293	36	14.32	1.00
	0.05	9.665	0.239	89	28.80	2.11
	0.10	9.645	0.284	174	58.88	4.52
	0.20	9.659	0.220	370	104.8	8.78
Wet-cured, 28 d	0	9.641	0.135	31	11.24	1.00
	0.01	9.673	0.175	35	11.40	1.02
	0.05	9.711	0.284	85	28.17	2.63
	0.08	9.709	0.275	111	37.62	3.61
	0.10	9.659	0.261	161	53.43	5.23
	0.12	9.680	0.262	167	56.71	5.65
	0.15	9.669	0.255	168	56.42	5.77
	0.20	9.659	0.261	220	71.09	7.59
Mixed-cured, 28 d	0	9.654	0.155	46	17.65	1.00
	0.01	9.679	0.183	82	23.76	1.36
	0.05	9.669	0.205	95	26.50	1.58
	0.08	9.657	0.286	109	37.93	2.32
	0.10	9.687	0.271	127	45.64	2.84
	0.12	9.679	0.239	162	50.00	3.17
	0.15	9.691	0.256	213	64.63	4.21
	0.20	9.686	0.248	300	90.95	6.18

Table 2
The integrated results of XRD diffraction peak of C_4AH_{13}

	P/C	d-value (Å)	FWHM (°)	Max. int.	Integ. int.	$\frac{\text{Integ.int.}(1+P/C)}{\text{Integ.int}_{P/C=0}}$
Wet-cured, 7 d	0	7.573	0.367	78	32.14	1.00
	0.05	7.553	0.339	110	48.03	1.57
	0.10	7.600	0.377	61	27.42	0.94
	0.20	–	–	–	0	0
Wet-cured, 28 d	0	7.553	0.332	511	174.49	1.00
	0.01	7.550	0.243	589	195.78	1.13
	0.05	7.587	0.240	523	176.59	1.06
	0.08	7.579	0.246	423	155.93	0.97
	0.10	7.568	0.261	355	131.78	0.83
	0.12	7.578	0.262	277	108.36	0.70
	0.15	7.568	0.274	204	77.48	0.51
	0.20	7.572	0.332	161	55.99	0.39
Mixed-cured, 28 d	0	7.558	0.248	469	156.95	1.00
	0.01	7.573	0.234	474	168.62	1.09
	0.05	7.566	0.267	379	146.22	0.98
	0.08	7.561	0.253	293	99.08	0.68
	0.10	7.570	0.312	239	85.42	0.60
	0.12	7.569	0.257	181	64.79	0.46
	0.15	7.587	0.307	125	41.85	0.31
	0.20	7.583	0.283	82	26.18	0.20

cement pates is easier to evaporate, which limits the cement hydration to some extent.

$$\text{Ca(OH)}_2 \text{ content } (\%) = \frac{\Delta H_P(1+P/C)}{\Delta H_{CH}} \times 100\% \quad (1)$$

Where ΔH_P is the enthalpy of decomposition reaction of Ca $(OH)_2$ in SBR-modified cement paste; ΔH_{CH} is the enthalpy of decomposition reaction of analytical pure $Ca(OH)_2$.

Table 3
The integrated results of XRD diffraction peak of $Ca_4Al_2Fe_2O_{10}$

	P/C	d-value (Å)	FWHM (°)	Max. int.	Integ. int.	$\frac{\text{Integ.int.}(1+P/C)}{\text{Integ.int}_{P/C=0}}$
Wet-cured, 3 d	0	7.297	0.238	361	86.33	1.00
	0.05	7.275	0.236	326	78.84	0.96
	0.10	7.291	0.186	359	83.52	1.06
	0.20	7.281	0.206	336	84.56	1.18
Wet-cured, 7 d	0	7.268	0.184	320	68.19	1.00
	0.05	7.268	0.205	280	58.69	0.90
	0.10	7.289	0.189	298	62.64	1.01
	0.20	7.284	0.201	290	74.52	1.31
Wet-cured, 28 d	0	7.288	0.222	225	51.72	1.00
	0.01	7.284	0.223	185	44.09	0.86
	0.05	7.311	0.191	234	51.24	1.04
	0.08	7.311	0.190	222	46.58	0.97
	0.10	7.294	0.200	211	48.13	1.02
	0.12	7.305	0.195	250	54.97	1.19
	0.15	7.295	0.191	257	58.50	1.30
	0.20	7.289	0.191	304	66.86	1.55
Mixed-cured, 28 d	0	7.286	0.214	253	55.45	1.00
	0.01	7.303	0.184	260	55.67	1.01
	0.05	7.299	0.234	221	49.26	0.93
	0.08	7.291	0.191	218	46.72	0.91
	0.10	7.293	0.202	241	50.45	1.00
	0.12	7.297	0.186	279	59.68	1.21
	0.15	7.302	0.184	294	63.18	1.31
	0.20	7.298	0.215	307	64.74	1.40

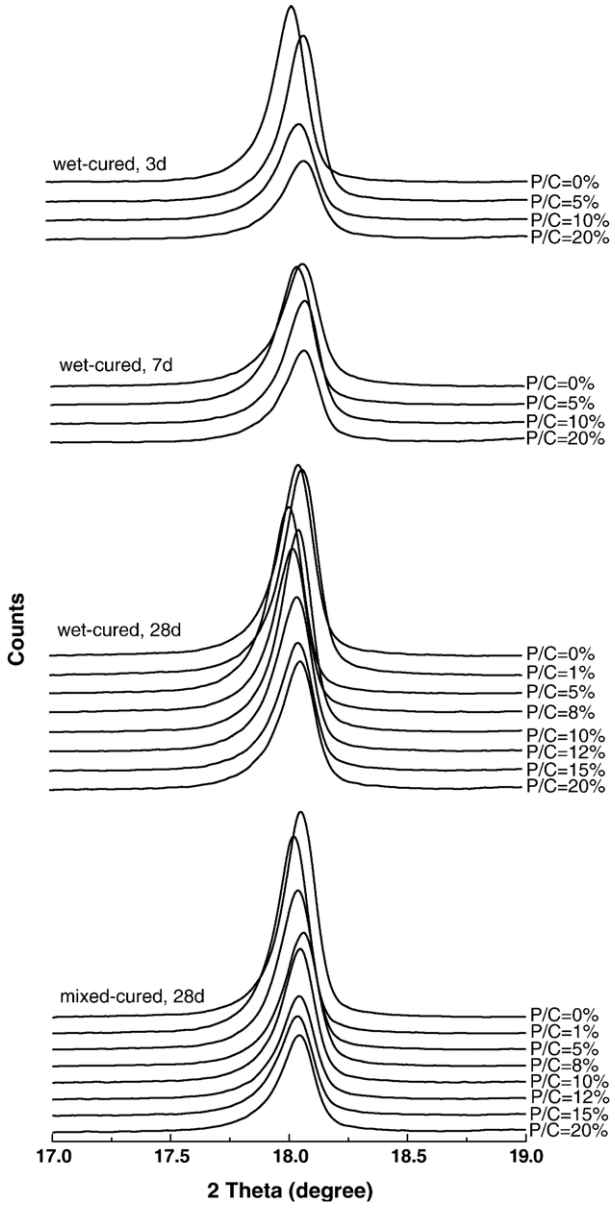

Fig. 4. XRD curves of SBR-modified cement pastes at 2θ range of 17–19°.

3.2. XRD analysis

Fig. 3 exhibits the XRD curves of SBR-modified cement pastes with different curing ages and P/C at 2θ range of 8–13°. The diffraction peak at about 9.1° strengthens with P/C, which relates to the diffraction of (100) crystal plane of ettringite [23]. The strengthening of the peak with P/C is more apparent at longer curing ages. The diffraction peak at about 11.6° is corresponding to the C_4AH_{13}. This peak is not observed at the XRD curves of the modified pastes hydrated for 3 d, implying no or only a little C_4AH_{13} in these systems. The diffraction peak becomes obvious with curing age, while weakens with P/C. The diffraction peak of (020) crystal plane of $Ca_4Al_2Fe_2O_{10}$ at about 12.1° fades with curing age, showing that the degree of cement hydration reinforces with hydration time.

Table 4
The integrated results of XRD diffraction peak of $Ca(OH)_2$

	P/C	*d*-value (Å)	FWHM (°)	Max. int.	Integ. int.	$\frac{\text{Integ.int.}(1+P/C)}{\text{Integ.int}_{P/C=0}}$
Wet-cured, 3 d	0	4.919	0.157	8784	1711.34	1.00
	0.05	4.906	0.161	8311	1655.77	1.02
	0.10	4.911	0.180	4824	1084.38	0.70
	0.20	4.905	0.181	3891	888.00	0.62
Wet-cured, 7 d	0	4.907	0.183	6243	1455.23	1.00
	0.05	4.913	0.174	6998	1504.52	1.09
	0.10	4.905	0.172	6248	1340.24	1.01
	0.20	4.906	0.183	4663	1014.27	0.84
Wet-cured, 28 d	0	4.910	0.169	9663	2020.20	1.00
	0.01	4.905	0.171	10,472	2216.98	1.11
	0.05	4.921	0.165	9503	1959.26	1.02
	0.08	4.917	0.166	8285	1700.45	0.91
	0.10	4.907	0.167	9147	1952.94	1.06
	0.12	4.912	0.188	7865	1680.78	0.93
	0.15	4.910	0.176	6499	1408.72	0.80
	0.20	4.908	0.175	6477	1417.01	0.84
Mixed-cured, 28 d	0	4.911	0.178	11,060	2370.23	1.00
	0.01	4.919	0.159	11,674	2284.11	0.97
	0.05	4.914	0.171	9375	1945.89	0.86
	0.08	4.909	0.174	7842	1678.51	0.76
	0.10	4.912	0.164	7864	1609.65	0.75
	0.12	4.913	0.173	6064	1313.96	0.62
	0.15	4.915	0.177	5841	1274.94	0.62
	0.20	4.913	0.170	5676	1222.71	0.62

In order to analyze the effect of SBR on the content of the cement hydrates quantitatively, the special diffraction peak of ettringite, C_4AH_{13} and $Ca_4Al_2Fe_2O_{10}$ are integrated using software MDI Jade 6.5, as listed in Tables 1–3. Table 1 shows the integrated results of XRD diffraction peak of (100) crystal plane of ettringite such as the *d*-value, the peak width at half height (FWHM), the maximal intensity (Max. int.), the integrated intensity (Integ. int.) and the ratio of the ettringite content in the modified paste to that in the control paste calculated from the integrated intensity. The integrated intensity of the diffraction peak of (100) crystal plane of ettringite of the modified pastes rises with *P*/*C* whatever curing age and method. When *P*/*C* is 20%, the content of the ettringite in the modified pastes wet-cured for 3 d, 7 d, 28 d and mixed-cured for 28 d reaches 3.24, 8.78, 7.59 and 6.18 times to that of the corresponding control paste, respectively. It indicates that SBR accelerates the formation and stability of ettringite, i.e., SBR promotes the reaction of calcium aluminate with gypsum in SBR-modified cement pastes.

The integrated results of the characteristic diffraction peak of C_4AH_{13} are displayed in Table 2. The integrated intensity of the diffraction peak enhances with *P*/*C* below 10%, 8% and 5% for the modified pastes wet-cured for 7 d, 28 d and mixed-cured for 28 d, respectively. After that, the integrated intensity of the peak depresses sharply with increasing *P*/*C*. When *P*/*C* is 20%, the characteristic diffraction peak of C_4AH_{13} is not observed at the XRD curves of the modified pastes wet-cured for 7 d. Moreover, the content of the C_4AH_{13} for the modified pastes wet-cured and mixed-cured for 28 d is down to 0.39 and 0.20 times to that of the corresponding control paste. It shows that an addition of a small quantity of SBR promotes the formation of C_4AH_{13}. On the other hand SBR restrains the formation of C_4AH_{13} at a large dosage.

Table 3 is the integrated results of the characteristic diffraction peak of $Ca_4Al_2Fe_2O_{10}$. From the ratio of the $Ca_4Al_2Fe_2O_{10}$ content of the modified paste to that of control paste, it is clear that the change of the $Ca_4Al_2Fe_2O_{10}$ content is not obvious with *P*/*C* below 10%, and then goes up slightly with growing *P*/*C*. When *P*/*C* is 20%, the $Ca_4Al_2Fe_2O_{10}$ content in the modified paste wet-cured for 3 d, 7 d, 28 d and mixed-cured for 28 d is 1.18, 1.31, 1.55 and 1.40 times to that of the corresponding control paste, respectively. It means that addition of SBR more than 10% delays the hydration reaction of $Ca_4Al_2Fe_2O_{10}$. That is to say, the degree of cement hydration declines.

The XRD curves of SBR-modified cement pastes with different curing ages and *P*/*C* at the 2θ range of 17–19° are displayed in Fig. 4. The diffraction peak at about 18° is ascribed to the diffraction of (001) crystal plane of $Ca(OH)_2$. In order to analyze the effect of SBR on the degree of cement hydration, software MDI Jade 6.5 is also used to integrate the diffraction peak quantitatively. As shown in Table 4, SBR raises the Ca $(OH)_2$ content to some extent when *P*/*C* is no more than 5%, 10% and 10% for the modified pastes wet-cured for 3 d, 7 d and 28 d, respectively. With further increasing *P*/*C*, the $Ca(OH)_2$ content declines. It shows that appropriate addition of SBR accelerates cement hydration reaction in SBR-modified cement pastes. The $Ca(OH)_2$ content in mixed-cured modified pastes goes down slowly with *P*/*C*, and the content is lower than that formed in wet-cured modified pastes. It suggests that wet cure is more helpful for cement hydration. The results are coherent with

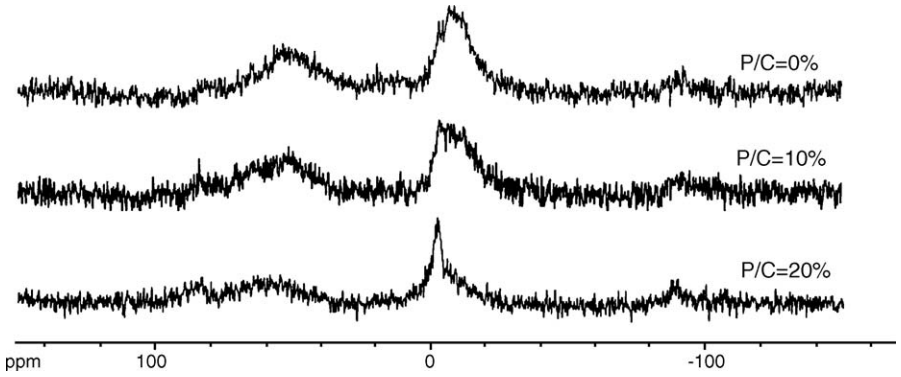

Fig. 5. ^{27}Al NMR spectra of SBR-modified cement pastes hydrated for 3 d.

that of DSC analysis. A previous paper showed that the strength of mixed-cured modified mortars is higher [19], which indicates that the strength of the polymer-modified mortars is influenced by both the cement hydration and the formed polymer film. Because it is well known that mixed cure is more helpful for the polymer film development [24].

3.3. ^{27}Al NMR analysis

Fig. 5 displays the ^{27}Al NMR spectra of SBR-modified cement pastes hydrated for 3 d with different *P*/*C*. Tetrahedron and octahedron are the forms of aluminum-oxide polyhedrons in the SBR-modified cement pastes from the appearance of the peaks at 50 ppm, corresponding to $[AlO_4]^{5-}$ tetrahedron, and at −8 ppm, corresponding to $[AlO_6]^{9-}$ octahedron. And the peak at − 8 ppm is stronger, indicating that the octahedron is prominent. The chemical shifts of both the $[AlO_4]^{5-}$ and $[AlO_6]^{9-}$ hardly change with *P*/*C* and curing time. Note that Al^{3+} still exists in tetrahedron after participating in the three dimensional structural net of $[SiO_4]^{4-}$, but its structural environment changes. There may be four $[SiO_4]^{4-}$ tetrahedrons or three $[SiO_4]^{4-}$ tetrahedrons and a $[AlO_4]^{5-}$ tetrahedron, or other modulating ions. The depression of the symmetry of structural environment results in the broadness of the peak of $[AlO_4]^{5-}$ tetrahedron at 50 ppm [25].

Similarly, the diversity of the structural environment of the $[AlO_6]^{9-}$ octahedron makes the peak at −8 ppm broad. With the increment of *P*/*C*, the peak for $[AlO_6]^{9-}$ octahedron at −8 ppm weakens and a sharp symmetric peak appears at −3 ppm. It means that the environment of the $[AlO_6]^{9-}$ octahedron becomes more homogeneous.

The ^{27}Al NMR spectra of SBR-modified cement pastes hydrated for 28 d with different *P*/*C* are laid in Fig. 6. The peak at −8 ppm corresponding to $[AlO_6]^{9-}$ octahedron at the ^{27}Al NMR spectra is sharper than that of the modified pastes hydrated for 3 d, which indicates that the structural environment symmetry of the $[AlO_6]^{9-}$ strengthens with hydration time. When *P*/*C* is 20%, the peak for $[AlO_6]^{9-}$ octahedron splits evidently; and a sharp symmetric peak appears at −3 ppm. It is seen that the sharp symmetric peak at −3 ppm becomes evident for the modified pastes with different curing ages. That may be some $[AlO_6]^{9-}$ octahedron separates from the three dimensional structure net of $[SiO_4]^{4-}$ tetrahedron and distributes outside of the net independently [25].

It can be drawn that the effect of a small SBR dosage on the structure of Al^{3+} in SBR-modified cement pastes is slight. However, the state of Al^{3+} in the modified pastes changes obviously and the combination of Al^{3+} with $[SiO_4]^{4-}$ tetrahedron is restrained at the addition of 15% SBR.

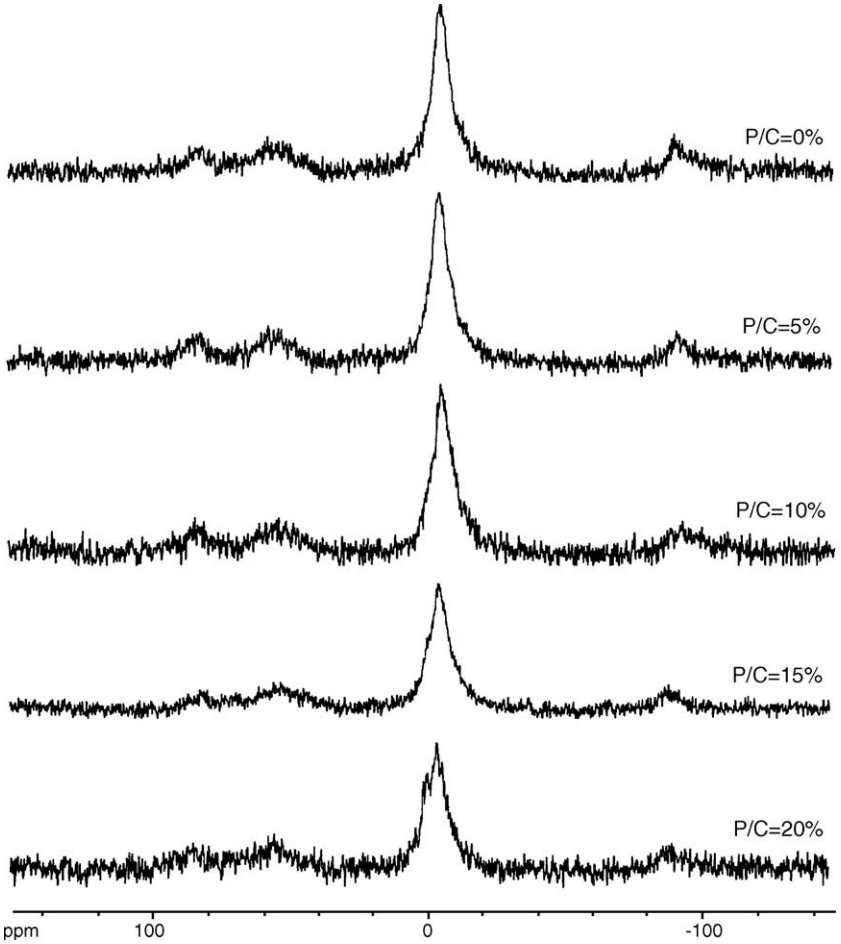

Fig. 6. ^{27}Al NMR spectra of SBR-modified cement pastes hydrated for 28 d.

3.4. ^{29}Si NMR analysis

The ^{29}Si NMR spectra of SBR-modified cement pastes hydrated for 3 d and 28 d are shown in Figs. 7 and 8, respectively. A sharp symmetric absorption peak at −67 ppm is observed at the ^{29}Si NMR spectra of the modified pastes hydrated for 3 d, which corresponds to the ^{0}Q, i.e. tetrahedron monomer structure of $[SiO_4]^{4-}$. Symmetric double absorption peaks at −75ppm and −76 ppm are found, which are ascribed to the ^{1}Q structure of $[SiO_4]^{4-}$ tetrahedron, i.e., the tetrahedron dimmer structure. Except for the same absorption peaks with the modified pastes hydrated for 3 d, a new absorption peak appears at −81 ppm at the ^{29}Si NMR spectrum of the modified pastes hydrated for 28 d. The peak is corresponding to the ^{2}Q structure of $[SiO_4]^{4-}$ tetrahedron, i.e., the three-tetrahedron polymer. Furthermore, the intensity of the double peaks corresponding to the ^{1}Q structure strengthens with hydration time. It is clear that the Si–O bond in SBR-modified cement pastes exists in $[SiO_4]^{4-}$ tetrahedron. C–S–H gel is formed with cement hydration, and the absorption peak of ^{0}Q structure weakens and the peaks of ^{1}Q and ^{2}Q structure enhance with hydration time. With the development of hydration, the $[SiO_4]^{4-}$ tetrahedron in C–S–H gel polymerizes to form dimer and three-tetrahedron polymer.

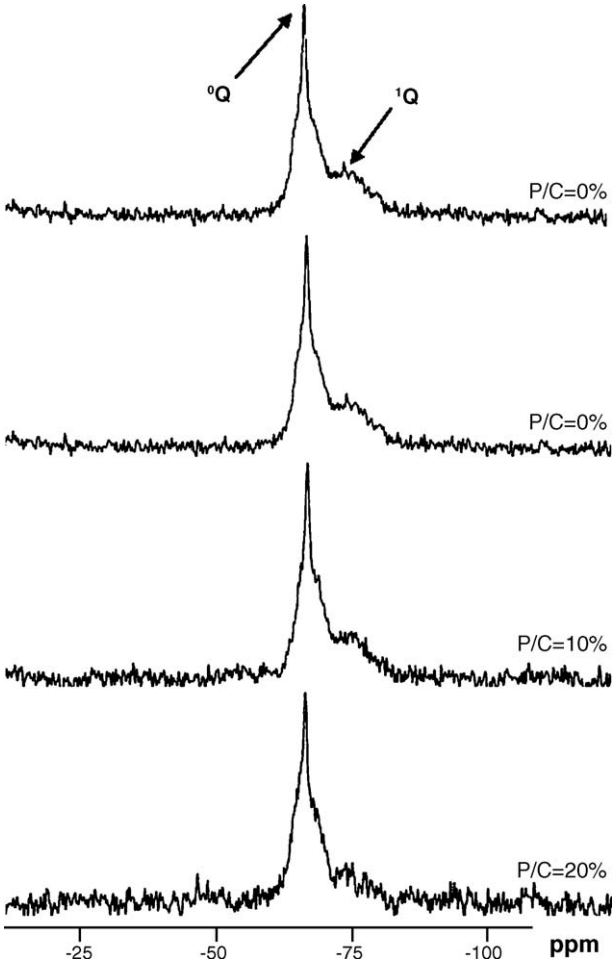

Fig. 7. ^{29}Si NMR spectra of SBR-modified cement pastes hydrated for 3 d.

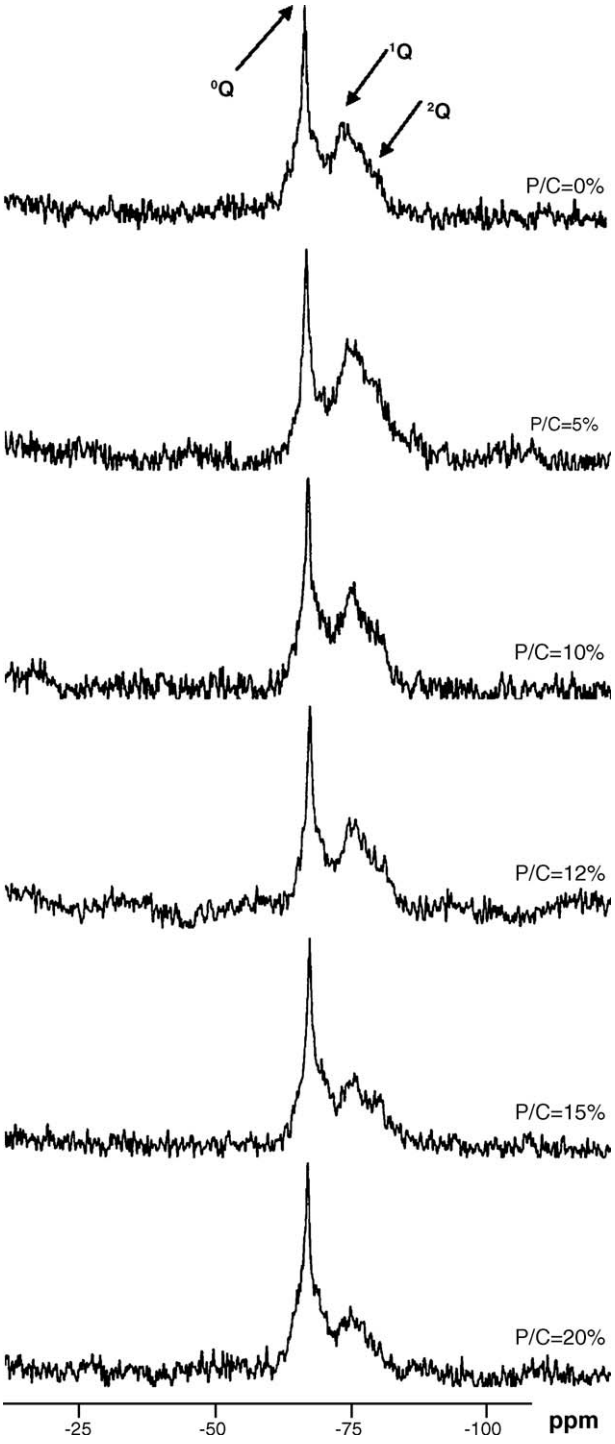

Fig. 8. ^{29}Si NMR spectra of SBR-modified cement pastes hydrated for 28 d.

It can be seen from the figures that the influence of SBR on the intensity of the absorption peak is not remarkable when *P*/*C* is below 12%. But with *P*/*C* above 12%, the absorption peaks of ^{1}Q and ^{2}Q structure weaken evidently, which indicates that the polymerization of $[SiO_4]^{4-}$ tetrahedron in C–S–H gel is affected and its polymerization degree depresses.

4. Conclusions

The content of $Ca(OH)_2$ in wet-cured SBR-modified cement pastes increases with *P*/*C* firstly and then declines after reaching a maximum, and in the longer hydration time the variation is more obvious. With wet cure, appropriate addition of SBR accelerates the cement hydration reaction, and the degree of cement hydration is maximal when *P*/*C* is 5%, 10% and 10% for the modified pastes hydrated for 3 d, 7 d and 28 d, respectively. While the influence of SBR on the $Ca(OH)_2$ content and the degree of cement hydration is slight in mixed-cured SBR-modified cement pastes. SBR promotes the reaction of calcium aluminate with gypsum and thus enhances the formation and stability of ettringite; meanwhile it restrains the formation of C_4AH_{13}. The $[AlO_4]^{5-}$ tetrahedron and $[AlO_6]^{9-}$ octahedron are the forms of aluminum-oxide polyhedrons in SBR-modified cement pastes, and the octahedron is prominent. The $[SiO_4]^{4-}$ is tetrahedron monomer or dimer structure in SBR-modified cement pastes hydrated for 3 d, and three-tetrahedron polymer appears in the modified pastes hydrated for 28 d. The effect of a small SBR dosage on the structure of Al^{3+} and $[SiO_4]^{4-}$ in SBR-modified cement pastes is slight. However, the combination of Al^{3+} with $[SiO_4]^{4-}$ tetrahedron is restrained with above 12% SBR addition, and some $[AlO_6]^{9-}$ octahedron separates from the three dimensional structural net of $[SiO_4]^{4-}$ tetrahedron. At the same time, the polymerization of $[SiO_4]^{4-}$ tetrahedron in C–S–H gel is affected and its polymerization degree depresses obviously.

Acknowledgment

This project was supported by the Special Fund for Major State Research Projects of China (2001CB610704) and China Postdoctoral Science Foundation (2004035489).

References

[1] S. Zhong, H. Yuan, Application of Polymer in Concrete, Chemistry and Industry Publishing Company, Beijing, Sep. 2003 (in Chinese).
[2] Y. Ohama, Recent progress in concrete-polymer composites, Adv. Cem. Based Mater. 5 (1) (1997) 31–40.
[3] Y. Ohama, Polymer-based admixture, Cem. Concr. Compos. 20 (2–3) (1998) 189–212.
[4] Y. Ohama, Principle of latex modification and some typical properties of latex-modified mortars and concretes, ACI Mater. J. 84 (1987) 511–518.
[5] E. Sakai, J. Sugita, Composite mechanism of polymer modified cement, Cem. Concr. Res. 25 (1) (1995) 127–135.
[6] M.U.K. Afridi, Y. Ohama, K. Demura, M.Z. Iqbal, Development of polymer films by the coalescence of polymer particles in powdered and aqueous polymer-modified mortars, Cem. Concr. Res. 33 (2003) 1715–1721.
[7] J. Long, K. Yu, G. Li, Interaction between polymer and cement hydrates, Concrete 3 (1995) 35–41 (in Chinese).
[8] N. Liang, Effect of the added styrene–butadiene latex on the hydration process of cement and the micro-morphology of hardened cement paste, J. Chin. Ceram. Soc. 22 (4) (1994) 340–346 (in Chinese).
[9] A. beeldens, J. monteny, W. Vincke, N. De Belie, D. Van Gemert, L. Taerwe, W. Verstraete, Resistance to sulphuric acid corrosion of polymer-modified mortars, Cem. Concr. Compos. 23 (2001) 47–56.
[10] J. Schulze, Influence of water–cement ratio and cement content on the properties of polymer-modified mortars, Cem. Concr. Res. 29 (1999) 909–915.
[11] Z. Xia, L. Luo, The impact of curing conditions on the mechanical properties of modified mortars and cement, J. S. China Univ. Technol. (Nat. Sci. Ed.) 29 (6) (2001) 83–86 (in Chinese).
[12] S. Hu, L. Luo, Study on mechanical properties of polymer-modified cement mortars, Technol. Road Traffic 2 (2002) 30–34 (in Chinese).
[13] S. Zhong, Z. Chen, Properties of latex blends and its modified cement mortars, Cem. Concr. Res. 32 (10) (2002) 1515–1524.
[14] S. Zhong, M. Shi, Z.H. Chen, The AC response of polymer-coated mortar specimens, Cem. Concr. Res. 32 (6) (2002) 983–987.
[15] J. Mirza, M.S. Mirza, R. Lapointe, Laboratory and field performance of polymer-modified cement-based repair mortars in cold climates, Constr. Build. Mater. 16 (6) (2002) 365–374.
[16] J. Do, Y. Soh, Performance of polymer-modified self-leveling mortars with high polymer–cement ratio for floor finishing, Cem. Concr. Res. 33 (10) (2003) 497–1505.
[17] P.M. Wang, Q. Xu, J. Stark, Mechanical properties of styrene–butadiene emulsion modified cement mortar used for repair of bridge surface, J. Build. Mater. 4 (1) (2001) 1–6 (in Chinese).
[18] F. Li, Study on properties of SBR-modified cement mortars at different water–cement mass ratio, Dissertation for master's degree of Tongji University, June 2003 (in Chinese).
[19] R. Wang, P.M. Wang, X.G. Li, Physical and mechanical properties of styrene–butadiene rubber emulsion modified cement mortars, Cem. Concr. Res. 35 (2005) 900–906.
[20] R. Wang, P.M. Wang, X.G. Li, Microstructural aspects of polymer-modified mortars using styrene–butadiene rubber (SBR) latex, Cem. Concr. Res. revised.
[21] H.G. Midgley, The determination of calcium hydroxide inset Portland cements, Cem. Concr. Res. 9 (1979) 77–82.
[22] B.E.I. Abdelrazig, D.G. Bonner, Estimation of the degree of hydration in modified ordinary Portland cement pastes by differential scanning calorimetry, Thermochim. Acta 145 (1989) 203–217.
[23] N. Yang, W. Yue, Handbook of a Collection of Illustrative Plates of Inorganic Nonmetal Materials, Wuhan University of Technology Publishing Company, Wuhan, Nov. 2000 (in Chinese).
[24] J. Feng, M.A. Winnik, R.R. Shivers, B. Clubb, Polymer blend latex films: morphology and transparency, Macromolecules 28 (1995) 7671–7682.
[25] X.J. Wang, Structure of aluminum-oxide polyhedron in fly ash before and after grinding studied by solid state NMR, Chin. J. Magn. Reson. 21 (2) (2004) 199–203 (in Chinese).